



In Silico Evaluation of Two Targeted Chimeric Proteins Based on Bacterial Toxins for Breast Cancer Therapy

Zoleikha Goleij ¹, Hamideh Mahmoodzadeh Hosseini ^{1, **}, Mohsen Amin ², Jafar Amani ¹, Elham Behzadi ³ and Abbas Ali Imani Fooladi ^{1, *}

¹Applied Microbiology Research Center, Systems Biology and Poisonings Institute, Baqiyatallah University of Medical Sciences, Tehran, Iran

²Department of Drug and Food Control, Faculty of Pharmacy and the Institute Pharmaceutical Sciences, Tehran University of Medical Sciences, Tehran, Iran

³Department of Microbiology, College of Basic Sciences, Shahr-e-Qods Branch, Islamic Azad University, Tehran, Iran

*Corresponding author: Applied Microbiology Research Center, Systems Biology and Poisonings Institute, Baqiyatallah University of Medical Sciences, Tehran, Iran. Tel/Fax: +98-2188068924, Email: imanifooladi.a@gmail.com

**Corresponding author: Applied Microbiology Research Center, Systems Biology and Poisonings Institute, Baqiyatallah University of Medical Sciences, Tehran, Iran, Email: hosseini361@yahoo.com

Received 2018 August 14; Revised 2019 January 16; Accepted 2019 January 16.

Abstract

Background: Despite major advances in cancer research, breast cancer still remains the most common cancer in women. Breast cancer is a heterogeneous disease, including at least 5 subtypes. Overexpression of human epidermal growth factor receptor 2 (HER2) in the patients denotes poor prognosis leading to a reduced survival rate compared to other subtypes of breast cancer. Therefore, HER2 can be a potential therapeutic target. To enhance the potency of HER2 blockers, the conjugation of specific cytotoxic agents with these types of anticancer agents may be successful. Application of antibody-based agents are important emerging anticancer therapies. One novel approach to increase the potency of monoclonal antibodies (mAbs) is combining them with toxic molecules.

Objectives: *Pseudomonas* exotoxin A (PE), ricin toxin (RT), and others in very minor quantities can be more potent and biologically active for this purpose.

Methods: In this study, we used trastuzumab as a ligand for HER2 receptor along with *Pseudomonas* exotoxin A (PE38) and A subunit of Shiga toxin 2a (Stx2a). This fusion protein selectively bound to the HER2 receptor. Upon uptake by the target cells, apoptosis and cell eradication was observed. An in silico method was used before the in vitro study to illustrate the properties and construction of the protein. Physicochemical properties, structure, stability, and ligand-receptor interaction of this chimeric protein were predicted by means of computational and bioinformatics tools and servers.

Results: The results of this study showed that codon adaptation index of s1 and p2 fusion gene has improved to 0.98 and .99, respectively. The mfold result has revealed that s1 and p2 mRNA were stable sufficient for efficient translation in the new host. Based on Ramachandran plot, s1 and p2 were categorized as constant fusion protein.

Conclusions: Finally, based on docking software analysis, the binding ability of Herceptin was robust enough to its receptor, so these constructs could be assigned as a new antitumor candidate in cancer therapy. The results suggested that s1 and p2 were stable fusion proteins with accurate affinity to the overexpressed receptors making them potential candidates for inducing apoptosis in breast cancer cells.

Keywords: Exotoxin A, Shiga Toxin, Herceptin, In Silico Modeling, Breast Cancer

1. Background

Despite major advances in cancer research, the breast cancer is the most common type of cancer among women worldwide. The molecular analysis indicates at least 5 subtypes of breast cancer and those patients overexpressing human epidermal growth factor receptor 2 (HER2) that includes nearly 15% to 20% of all breast cancer (BC) patients, are implicated with poor prognosis leading to a reduced survival rate compared to other subtypes of breast cancer

(1). HER2 is a member of human epidermal growth factor receptor (EGFR) family, which can dimerize with itself or other HER family members and is unique in that it lacks a known ligand. However, HER2 in a certain conformation is permanently accessible to heterodimerize with other family members such as HER1, HER3, and HER4 (2, 3) and it is optionally involved in dimer formation with EGFR family. Subsequent dimerization, the intracellular domains of the receptors interacts, and autophosphorylation of tyrosine

kinase occurs induce signal transduction pathways of cell proliferation, angiogenesis, metastasis, and apoptosis (4). Besides being a biomarker, HER2 is considered as a therapeutic target. During the past decade treatments that exactly targeted HER2, it significantly enhanced survival of patients with HER2-positive breast cancer (1). Screening of highly potent anticancer agents is important in this field.

Application of antibody-based therapies are emerging anticancer strategies (5). Use of hundreds of monoclonal antibodies (mAbs) is on the rise in this field (6). Trastuzumab was the first humanized monoclonal antibody targeted against HER2. This drug is currently used in controlling patients with metastatic breast cancer (7, 8). The antitumor activity of trastuzumab has not been entirely determined. Trastuzumab induces the induction of antibody dependent cell mediated cytotoxicity (ADCC), attenuated DNA repair, prevention of cleavage of HER2 extracellular domain (ECD), declined intracellular signal transduction, and anti-angiogenic consequences have been attributed to the administration of this medication (9). However, the efficacy of trastuzumab is not ideal, having many side effects, including cardiovascular adverse events, hypotension, leukopenia, anemia, dyspnea, fatigue, fever, headache, diarrhea, and skin rash.

The recurrence rate following the treatment with trastuzumab in female patients is about 15%, which may be related to *de novo* or acquired resistance to trastuzumab, requiring further investigations (10). It has been shown that use of mAbs alone may not be adequately effective, and they, consequently, are commonly combined by chemotherapy (11). One approach to increase the potency of mAbs is to conjugate antibody or antibody fragment to the toxic proteins forming chimeric proteins known as immunotoxins (5). mAbs are used for targeting and they bind to target receptor and then toxin moiety delivered to cell. For example, SS1 (dsFv) PE38 recombinant immunotoxin contains the variable domains of murine mAb SS1 that fused to PE38. SS1 mAb binds with high affinity to mesothelin in ovarian and pancreatic cancers (12). The toxins used in immunotoxins include plant or bacterial toxins. Certain toxins can inhibit protein synthesis upon internalization into the target cell. For example, *Pseudomonas* exotoxin A (PE), ricin toxin (RT), and other similar toxins are more potent in low quantities (5).

In this study, we used trastuzumab as a ligand for HER2 receptor conjugated to *Pseudomonas* exotoxin A (PE38) and a subunit of Shiga toxin 2a (Stx2a). This fusion protein selectively binds to HER2 receptor and eradicates the target cells upon uptake.

PE has commonly been used as a cytotoxic segment in targeted cancer therapy. It is a bacterial toxin originally been synthesized by *Pseudomonas aeruginosa* as a 69 kDa

polypeptide before being processed through deletion of a N-terminal 25-residue to secrete a 66 kDa native toxin (13). PE is a member of AB toxin family composed of 3 main functional domains: (1) a receptor binding (R) domain (domain I) that facilitates the attachment of toxin to the specific receptors. (2) The B subunit consisting of a translocation (T) domain (domain II) that promotes the transport of the A subunit into the cytoplasm; and (3) The A (domain III) subunit that encodes the catalytic (C) domain with cytotoxic activity. Catalytic domain catalyzes the inactivation of eEF2 by transferring an ADP-ribosyl group from NAD⁺ to diphthamide residue. Domain III needs a quota of domain Ib for exerting complete catalytic activity (14, 15). Therefore, amino acid sequence of domain III is from 395 to 613 (16).

Shiga toxins (Stx), the main virulence factors of Stx-producing *Escherichia coli* (STEC), are members of AB5 family of toxins consisting of an A subunit, which has enzymatic activity and 5 equal B subunits (7.7 kDa) for binding to cellular receptors (17). Each B subunit anchors 3 distinguishing binding sites that exactly interacts with trisaccharide subunit of the glycosphingolipid Gb3 (18). Then, the A subunit (32.2 kDa) is cleaved by the furin protease to A1 fragment and a small A2 fragment (19). In the cytoplasm, A1 fragment cleaves the N-glycosidic bond of adenine-4324 in 28S rRNA and inhibits tRNA adhesion, which prevents protein synthesis (20). Stx comprises 2 main antigenic forms (Stx1 and Stx2). Stx2 is 100 times more potent than Stx1 in mouse models (21). Stx2 is classified to subtypes Stx2a-Stx2g based on nucleotide and amino acid sequence.

Using an in silico approach, we designed 2 chimeric constructs composed of PE38 (domain Ib-domain II)-VL-VH and Stxa-PE38 (domain Ib-domain II)-VL-VH sequences conjugated to antibody and anticipated these chimeric constructs induce apoptosis and eliminate breast cancer cells. The chimeric genes were optimized to produce the protein in a prokaryotic expression system. High yield of protein expression was related to the ability of chimeric gene to be expressed properly and confirmed the validity of bioinformatic analysis. Ultimately, the refined chimeric protein was used for the evaluation in vitro and in vivo.

2. Methods

2.1. Design the Construct and Gene Optimization

The sequence of PE38, Stxa, and Herceptin were obtained from GeneBank. The sequences of the constituents of chimeric construct were PE (accession No. P11439), Stx2a (accession No. P09385). Recombinant constructs were generated by fusing the toxins with antibody (VL-VH of Herceptin), using a linker. Several hydrophobic linkers were tested by the GOR4 tool (22) to separate 2 functional parts

of the chimeric protein with or without minimal intrusion in their native secondary structure (data not shown). PE38 (domain Ib-domain II-domain III)-VL-VH and Stxa-PE38 (domain Ib-domain II)-VL-VH sequences were created by fusing the N-terminal of PE38, the C-terminal of VL (PE38-VL-VH), N-terminal of PE38, and the C-terminal of Herceptin (Stxa-PE38-VL-VH), using hydrophobic ASGGPE amino acid linker. GGGGSGGGGSGGGGS amino acid linker was used between VL and VH.

The new chimeric protein constructs were back-translated and optimized based on bacterial expression host, *E. coli*. Codon usage was checked by java codon optimization tool (JCat) (<http://www.jcat.de/>), optimizer web server (23, 24), and gene script server (<http://www.genscript.com/>). GC percentage and codon adaptation index (CAI) were, then, calculated (25).

The in silico multiparameter chimeric gene optimization and gene analysis of the synthetic chimera genes were completed, using online data bases such as the codon database, Genbank codon usage database, Swissprot reverse translation online tool (25), and stand-alone software such as DNASIS software.v2.0 (Hitachi Software Engineering, Yokohama, Japan), Leto software v1.0 (Entelechon, GmbH, Germany), and the software Protein2DNA (DNA 2.0, www.dnatwopointo.com). The chimeric genes were synthesized by Biomatic Company.

2.2. mRNA Structure Prediction

The program **mfold** was recruited to analyze the messenger RNA (mRNA) secondary structure of the chimeric genes.

2.3. Protein Primary Structure Property

The ExPasy ProtParam server (<http://us.expasy.org/tools/protparam.html>) was used to measure the physicochemical criteria, molecular weight, half-life, the isoelectric point (pI), instability index (II), the number of positive and negative residues in the sequence, extinction coefficient (ϵ), aliphatic index (AI), and grand average hydropathy (GRAVY) (26).

2.4. Protein Secondary Structure Prediction

GOR secondary structure prediction method version IV was used to predict the secondary structure of the proteins (27). In addition, the predict protein server was used to estimate the protein structure and sequence analysis and to predict the functional properties of the protein such as investigating regions missing regular structure, secondary structure, coiled-coil structure, regions with low-complexity, the solvent accessible surface area (SASA), transmembrane (TM) helices, and location of disulfide bridges in a protein.

2.5. 3D Structure Prediction Using Homology Approach

The I-TASSER online server was used to produce the 3D model of the recombinant proteins (28) and their confidence score (C-score) is computed, showing the quality of predicted structure. In addition, Swiss-PdbViewer (aka DeepView) was recruited to analyze the stability of 3D structure of synthetic protein for energy minimization (29). The online program ASA was used for evaluation of solvent accessibilities of the protein residues (30).

2.6. Evaluation of Model Stability

Swiss PDBViewer, which includes a version of the GRO-MOS96 43B1 force field, was used for energy minimization and ProSA-web, Z-scores, and Procheck Ramachandran plot were used to assess the structure and to analyze stereo chemical configurations (31). Also, Swiss-PdbViewer (aka DeepView) was recruited to superimpose the query and template structure in order to visualize the generated models.

2.7. Ligand-Receptor Docking Using Hex

The docking of chimeric proteins with HER2 was done, using GRAMM-X Protein-Protein Docking Web Server v1.2.0., to study protein-ligand interactions and explore the application of the models for ligand binding potency prediction.

3. Results

3.1. Sequence Analysis and Construct Design

The nucleotide sequence of PE and Stx was obtained from online gene banks and fused to Herceptin. Several hydrophobic linkers were tested to select the best linker to maintain functionality and recover the normal structure of 3 parts of the recombinant protein (data not shown). Eventually, ASGGPE sequence was selected as the optimal linker between the toxin and antibody, and GGGGSGGGGSGGGGS sequence was selected as the linker between VL and VH of Herceptin (Figure 1).

Afterwards, the amino acid sequence (557aa for s1 and 601aa for p2) was back-translated and nucleic acid codons were optimized based on the codon labeled *E. coli* as the expression host. The codon usage bias in *E. coli* was enhanced by raising GC content and CAI for s1 to 53.74 (GC% of *E. coli* is about 50) and 0.98, respectively.

The codon usage bias in *E. coli* was elevated by raising GC content and CAI for p2 to 56.2 (GC content of *E. coli* is about 50) and 0.99, respectively.

A**B**

Figure 1. Schematic model shows the construct of Stx and IB + II of exotoxin bound to Herceptin by ASGGPE and vl and vh of Herceptin bound together by GGGGSGGGGSGGG linker. s1 (A) and p2 (B).

3.2. mRNA Structure Prediction

For determination of the probable folding of the chimeric gene, prediction of mRNA secondary structure has combined with comparative sequence analysis. The folding of 5' terminal region of the gene was similar to the bacterial gene structures. The minimum free energy (NFE) for RNA secondary structure was calculated. Values for s1 were $\Delta G = -599.20$ kcal/mol (Figure 2A) and $\Delta G = -663.00$ for p2 (Figure 2B).

The folding of the RNA construct for both new chimeric protein was presented here, which was in accordance with all 50 structural components that have been predicted in the study. The mRNA construct was quite stable to be translated sufficiently in the new host.

3.3. Primary Structure Property

The physicochemical properties of a s1 and p2 protein sequence were found out by ProtParam and are summarized in Table 1.

N-terminal end of the s1 sequence starts with glutamic acid (E or Glu). The half-life of this protein is estimated to be 1 hour in mammalian reticulocytes, in vitro, 30 minutes in yeast, in vivo, and more than 10 hours in *E. coli*, in vivo.

The N-terminal end of the p2 sequence starts with methionine (M, Met). The half-life of this protein is assessed to be 30 hours in mammalian reticulocytes, in vitro, more than 20 hours in yeast, in vivo, and more than 10 hours in *E. coli*, in vivo.

3.4. Protein Secondary Structure Prediction

The online software was used to predict the secondary structure of the s1 chimeric protein and the frequency of random coils were 49.19%, the extended strands were 24.06%, and alpha helices were less frequent and found to be about 26.75%. This is represented graphically in Figure 2C.

Moreover, the prediction of the secondary structure of the p2 chimeric protein was achieved, using online software and the frequency of random coils was 54.91%, extended strands were 19.47%, and alpha helices were less frequent and found to be about 25.62%. This is represented graphically in Figure 2D.

3.5. Tertiary Structural Prediction for the Chimeric Protein

3D models of chimeric protein have been created by I-Tasser, uploaded to the Swiss-PdbViewer server to describe the tertiary structural illustrations (32).

Five probable tertiary structures were anticipated by I-TASSER tool for s1 (Figure 3A). Consistent with C-scores calculated by this software, model 1, with a C-score of -2.71, had the maximum confidence between the other four models. The expected TM-score and RMSD were 0.40 ± 0.14 and 14.3 ± 3.8 Å, respectively. Also, 5 probable tertiary structures were predicted for p2 construct and model 3 with C-score of -1.98 was selected (Figure 3B). The TM-score and RMSD were 0.30 ± 0.10 and 17.6 ± 2.5 Å, respectively.

3.6. Evaluation of Model Stability

The spdbv (Swiss-PdbViewer) was employed to calculate the profile of energy minimization -6107.159 Kcal/mol

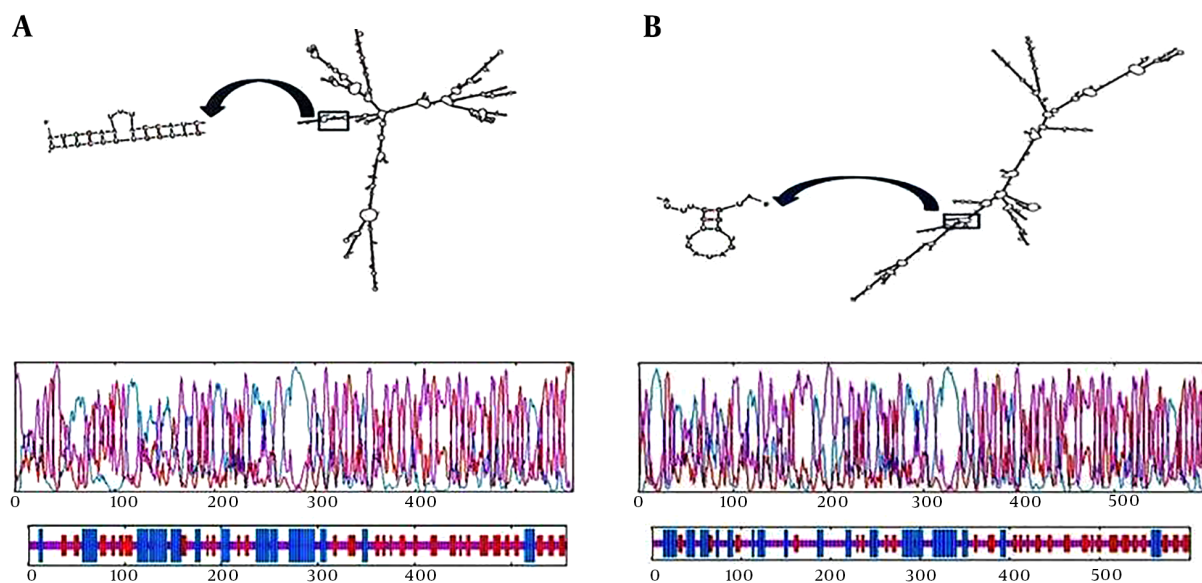


Figure 2. mRNA secondary structure prediction. $\Delta G = -599.20$ kcal/mol was for s1 (A) and $\Delta G = -663.00$ was for p2 (B). Graphical representation of secondary elements in chimeric proteins for s1 (C) and for p2 (D). Blue, purple, and red indicate helix, extended strand, and random coiled structures, respectively.

Table 1. Physicochemical Properties of s1 and p2 Sequence

Construct Name	S1	P2
Amino acids residues	557	601
Molecular weight	59873.40	64328.51
Isoelectric pointed	5.65	5.33
Maximum number of amino acids	Serine (S) + glycine (G)	Gly (G) and Ala(A)
Minimum number of amino acids	Glutamic acid and aspartic acid	Pyl (O) and Sec (U)
Total number of negatively charged residues (Asp + Glu)	51	65
Total number of positively charged residues (Arg + Lys)	42	53
Instability index (II)	40.40	41.81

and -6205.140, respectively for s1 and p2, indicating that the recombinant proteins had acceptable stability. Furthermore, according to Ramachandran plot analysis (Figure 4A and B), the stability of chimeric protein structure was approved.

3.7. Ligand Docking

Docking was performed by GRAMM-X server. This server could calculate protein ligand docking. We have uploaded a pair of HER2 and s1-Herceptin fusion protein as a ligand structures in PDB format in GRAMM-X server. Default parameters have been used for carrying out the jobs. When we have viewed the visualization tool like SPVBV, the docking between receptors of proteins and the ligand could be clearly observed as shown in Figure 4C and D.

4. Discussion

Breast cancer is the most common type of cancer among female adults of different age and race and the selected treatment strategy is of great importance to obtain the eligible result. Patients with overexpressed HER2 have shown weaker prognosis and reduced survival rate comparing to other breast cancer subtypes (1). mAbs that targeted tumor cell surface antigens have been displayed to prevent tumor cell growth (33). Also, cytotoxic potential can be enhanced through conjugating cytotoxic agents to mAbs (34). mAbs can bind to the extracellular domain of the human HER2 protein (35). The limitations of therapeutic potential of intact mAbs include large size and their immunogenicity. The Fv (antigen binding domain) of the an-

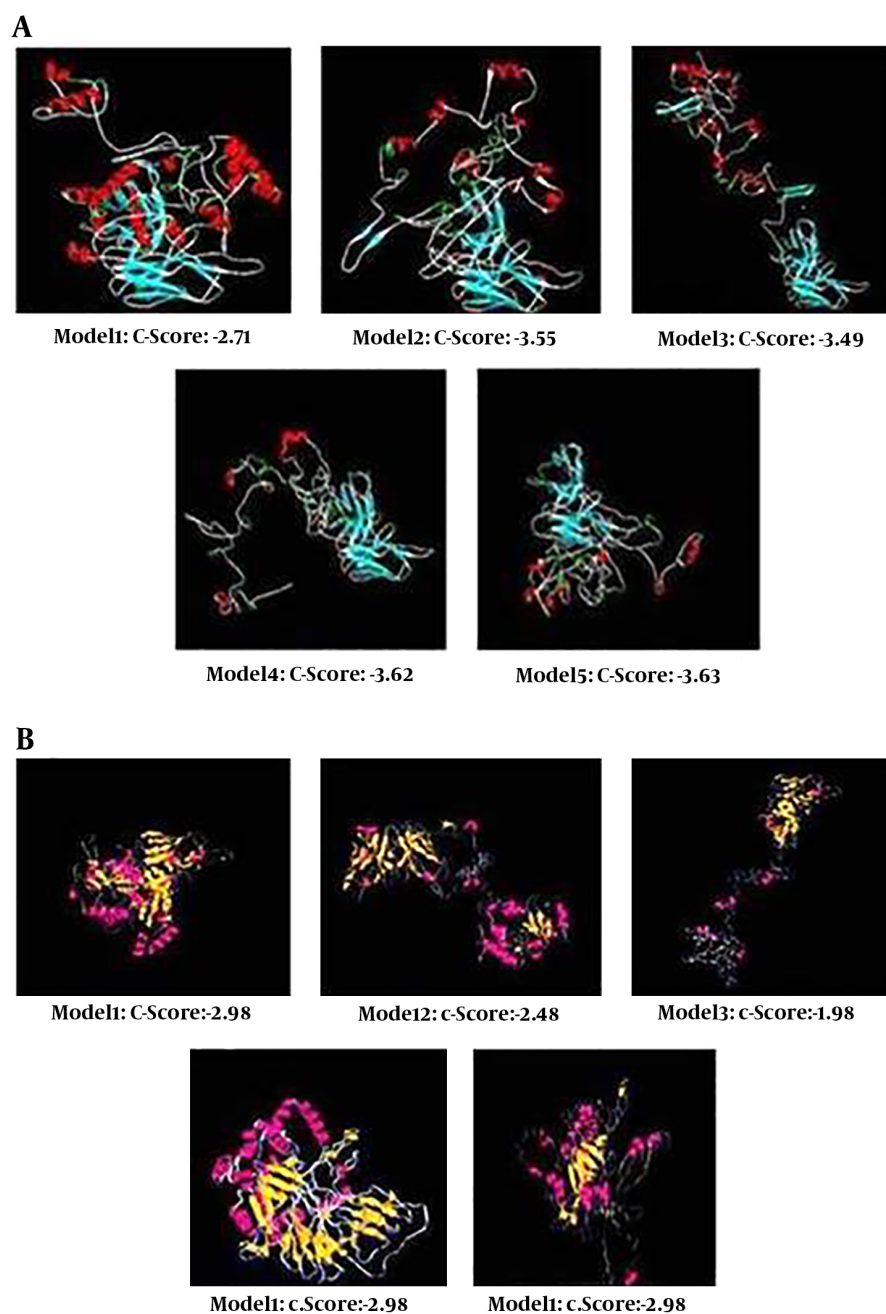


Figure 3. I-TASSER server was used to predict the tertiary structure of s1 and p2 chimeric proteins. Based on C-scores, the model 1 for s1 have a high confidence between other models (A) and model 5 for p2 have a high confidence between other models (B).

tibody may be adequate for binding to receptor. Single-chain antigen-binding proteins (scFv), created by a short peptide linker that attaches light (VL) and heavy chain (VH) variable domains of antibody, can be expressed in bacteria and they preserve their high-affinity binding to the target

(36). To increase the antibody efficacy, it can be conjugated to toxic agents. In this study, we designed 2 unique constructs, including stxa + Ib + II + vl + vh of Herceptin and III + Ib + II + vl + vh and compared their efficacy in silico to be introduced as new antitumor candidates. Previously

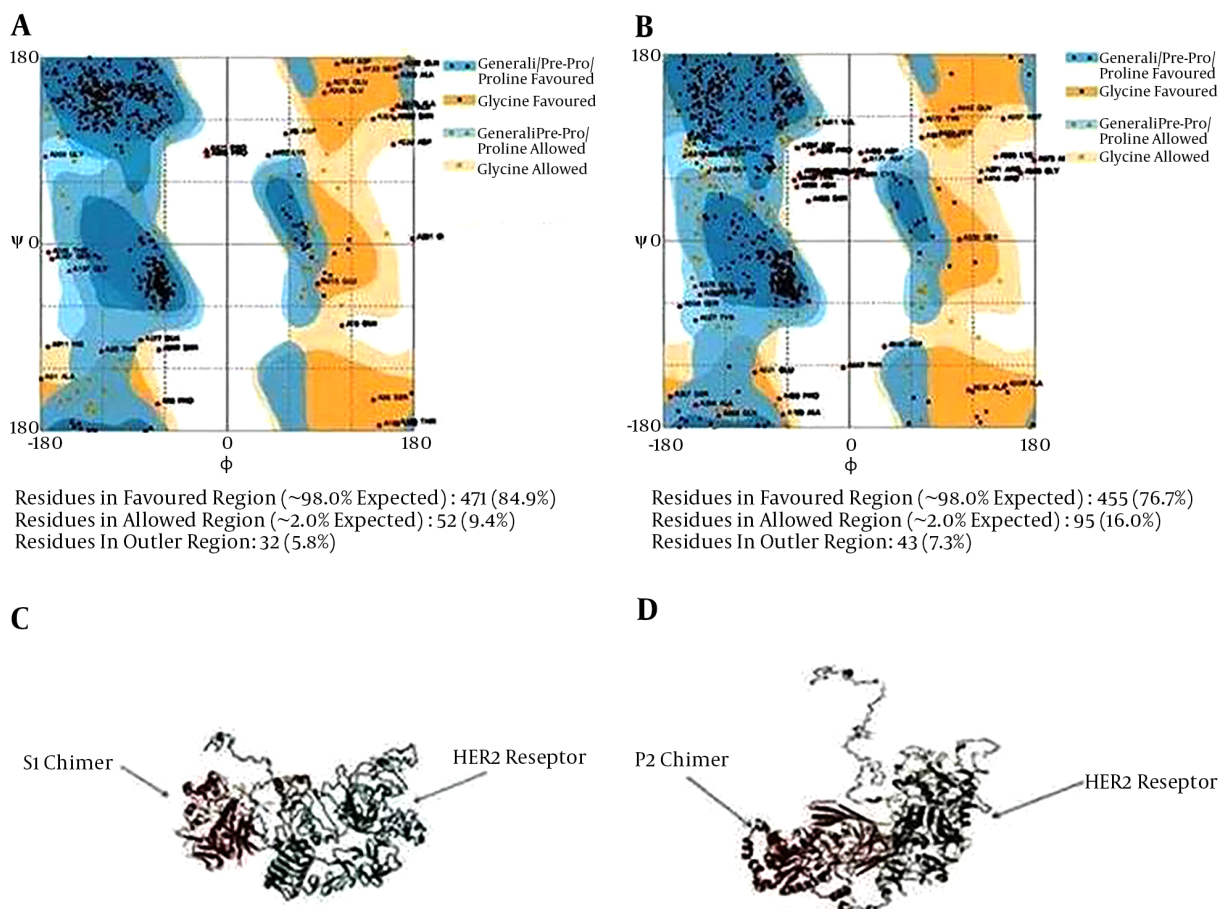


Figure 4. Evaluation of model stability based on a Ramachandran plot for s1 (A) and p2 (B). Docking of s1 chimeric protein with HER2 receptor (A) and p2 chimeric protein with HER2 receptor (B), using GRAMM-X. The models for ligand binding potency have been predicted to examine the protein-ligand interactions.

Keshtvarz et al. designed and evaluated PE38 - P4A8 chimer immunotoxin that was optimized by codon Adaptation index 0.94 and GC percentage 54.2, and revealed high and stable expression in bacterial cells. The most second structures were random coils and disordered regions; also, secondary structure of this immunotoxin was stable. The construct was hydrophilic and acidic. Tertiary structure of the fusion protein by C-score -3.36 contained the highest C-score. In this study, ASGGPE and (G4S)₃ linkers were used to isolate different segments (37). In another study, we designed and analyzed TGF α L3-SEB fusion protein that were optimized by CAI index 0.85 and by GC content 44.06% the overall stability of mRNA increased. The coil structural content was high. TGF α L3-SEB fusion protein was hydrophilic and the computed isoelectric point was 7.72. Tertiary structure of the fusion protein by C-score -0.42 contained the highest C-score (38). Comparing these two chimer proteins proposed that TGF α L3-SEB and PE38-P4A8

were stable fusion proteins with proper affinity to their receptors that overexpressed in cancer cells.

Our structural models could demonstrate that the attachment of the scFv domain to HER2 found on the surface of breast cancer cells uptake leads to the uptake of the structure by receptor-mediated endocytosis. Subsequently, the enzymatic domain of the structure is released into the cytoplasm of the cell and the elongation factor 2 is ADP-ribosylated. These events cause inactivation of elongation factor 2 by toxin, which inhibit the synthesis of the protein, leading to tumor cell death by apoptosis. Computational studies were done to predict physicochemical properties, structures, stability, and ligand-receptor interaction of these chimeric proteins. Several hydrophobic linkers were tested by the GOR4 tool (22) to separate 2 functional parts of the chimeric protein with or without minimal intrusion in their native protein secondary structure.

Recombinant stx + Ib + II + vI + vH and III + Ib + II + vI

+vh sequences were constructed by fusing the N-terminal of II and the C-terminal of VL (stxa + Ib + II + vl + vh) and N-terminal of II and the C-terminal of VL (III + Ib + II + vl + vh), using hydrophobic ASGGPE amino acid linker. The 12 aa-linker GSGGSGSGGSG was used for connection of VL and VH of the 2 proteins. Aria et al. reported the multimerizing feature of short helical linker paralleled with longer ones. Also, a flexible linker based on shorter conformation shows a proficient part in comparison to those with the helical linker (39).

The folding of the 2 structures (stxa + Ib + II + vl + vh) and (III + Ib + II + vl + vh) was analyzed and the 2 constructs have displayed accessible area and have not been hidden in their structure. In silico investigations have confirmed proficient transcriptional and translational capabilities, in addition to the quality expression of the new chimeric constructs in host expression vectors. The major factor used for gene optimization was CAI, with a range of 0 to 1 and an ideal value of 1.0. Since *E. coli* was used as the expression system codon usage table of *E. coli* was employed for back-translating the sequences and determining the optimum expression of the fusion proteins.

CAI in the wild type sequences was raised from 0.5 to 0.95 in the s1 optimized chimeric gene and 0.99 for p2. Moreover, the overall GC content was reduced from 65 to 53.74% for s1 and 68 to 57.5% for p2 that in turn enhance the stability of mRNA molecules, which has a major role in regulating synthetic gene expression. Furthermore, the required restriction enzyme sites were added to the ends of the designated gene for future assays. Codon optimization assured that synthetic construct was expressed optimally in the desired host vector. In this study, the mRNA structure was optimized based on the measure of Gibbs free energy (ΔG°) and the energy of the start codon in the mRNA, which is associated to the ribosome binding and translation initiation. The program mfold was recruited to assess the mRNA secondary structure of the s1 and p2 chimeric genes with the factors as follow: Linear RNA folding at 5%, window = 12, max folds = 50. All 43 structural elements achieved in this investigation have shown folding of the RNA construct at 37°C with initial ΔG ranging from -599.20 to -567.05 kcal/mol for s1 and -663.00 to -650.27 kcal/mol for p2. The best structure for s1 and p2 were -599.20 and -663.00 kcal/mol, respectively. The data have revealed the mRNA was stable sufficient for proficient translation in the new host.

The GOR method was applied for prediction of the secondary structure of 2 chimeric proteins. This software permits approximating the probable secondary structure of each amino acid together with its effect on the condition and structure of neighboring amino acids. The most plentiful structure within our fusion proteins was a random

coil that could be owing to the attendance of a high quantity of hydrophobic amino acids such as glycine. According to the results of this study, from the physicochemical feature analysis, both fusion proteins had acidic nature with high extinction coefficient at 280 nm owing to high content of cysteine, tryptophan, and tyrosine. The analysis of these fusion proteins could be performed by ultraviolet-visible spectrophotometry. Although our fusion proteins are partially unstable, its estimated high aliphatic index is attributed to protein stability in a broad range of temperatures.

One important factor in designing novel chimeric proteins is their molecular functions of supported by three-dimensional (3D) structure. The I-TASSER online server was used to produce the 3D model of the recombinant s1 and p2 protein based on their C-score, Z-score, RMSD, and TM-score. Five models were suggested by this server for each chimeric protein. For s1 and p2 proteins model 1 and model 3 had the highest C-score and were selected for further examination. Structural evaluation and the stability of the fusion protein were completed, using Procheck Ramachandran plot. Energy minimization was determined, using analysis of 3D structural stability of the chimeric proteins by using Swiss-PdbViewer.

Ligand-receptor docking was used to study whether Herceptin could reserve its binding ability to bring PE and Stx to tumors overexpressing HER2 (EGFR in many human tumors). Molecular docking was done by GRAMM-X server. A significant feature of GRAMM is the capability to smooth the protein surface demonstration to account for probable conformational alteration upon binding within the rigid body docking method.

S1 and p2 have revealed great affinity towards HER2. The results of the present study showed that the binding ability of s1 and p2 were strong enough to their receptor; so, s1 and p2 can be introduced as a novel antitumor candidate in breast cancer.

In conclusion, based on docking software analysis, the binding ability of Herceptin was robust enough to its receptor, so these constructs could be assigned as a new antitumor candidate in cancer therapy. The results suggested that s1 and p2 were stable fusion proteins with accurate affinity to the overexpressed receptors making them potential candidates for inducing apoptosis in breast cancer cells.

Acknowledgments

This paper was extracted from thesis.

Footnotes

Authors' Contribution: Zoleikha Goleij: Main writing and bioinformatic analysis. Abbas Ali Imani Fooladi: Designing idea, bioinformatic analysis and supervision of research. Hamideh Mahmoodzadeh Hosseini: Adviser, bioinformatic analysis and writing. Elham Behzadi: Editing and revision. Mohsen Amin: Writing editing and revision. Jafar Amani: Adviser in bioinformatic analysis.

Conflict of Interests: Authors declare that there is no conflict of interest.

Financial Disclosure: None declared.

Funding/Support: This work was supported by the grant from the Baqiayatallah University of Medical Sciences, Tehran, Iran.

References

- Li SG, Li L. Targeted therapy in HER2-positive breast cancer. *Biomed Rep.* 2013;1(4):499–505. doi: [10.3892/br.2013.95](https://doi.org/10.3892/br.2013.95). [PubMed: [24648975](https://pubmed.ncbi.nlm.nih.gov/24648975/)]. [PubMed Central: [PMC3917005](https://pubmed.ncbi.nlm.nih.gov/PMC3917005/)].
- Ross JS, Fletcher JA, Bloom KJ, Linette GP, Stec J, Symmans WF, et al. Targeted therapy in breast cancer: The HER-2/neu gene and protein. *Mol Cell Proteomics.* 2004;3(4):379–98. doi: [10.1074/mcp.R400001-MCP200](https://doi.org/10.1074/mcp.R400001-MCP200). [PubMed: [14762215](https://pubmed.ncbi.nlm.nih.gov/14762215/)].
- Schechter AL, Stern DF, Vaidyanathan L, Decker SJ, Drebin JA, Greene MI, et al. The neu oncogene: an erb-B-related gene encoding a 185,000-Mr tumour antigen. *Nature.* 1984;312(5994):513–6. [PubMed: [6095109](https://pubmed.ncbi.nlm.nih.gov/6095109/)].
- Yarden Y, Sliwkowski MX. Untangling the ErbB signalling network. *Nat Rev Mol Cell Biol.* 2001;2(2):127–37. doi: [10.1038/35052073](https://doi.org/10.1038/35052073). [PubMed: [11252954](https://pubmed.ncbi.nlm.nih.gov/11252954/)].
- Becker N, Benhar I. Antibody-based immunotoxins for the treatment of cancer. *Antibodies.* 2012;1(1):39–69. doi: [10.3390/antib1010039](https://doi.org/10.3390/antib1010039).
- Reichert JM. Antibody-based therapeutics to watch in 2011. *MAbs.* 2011;3(1):76–99. [PubMed: [21051951](https://pubmed.ncbi.nlm.nih.gov/21051951/)]. [PubMed Central: [PMC3038014](https://pubmed.ncbi.nlm.nih.gov/PMC3038014/)].
- von Minckwitz G, du Bois A, Schmidt M, Maass N, Cufer T, de Jongh FE, et al. Trastuzumab beyond progression in human epidermal growth factor receptor 2-positive advanced breast cancer: A german breast group 26/breast international group 03-05 study. *J Clin Oncol.* 2009;27(12):1999–2006. doi: [10.1200/JCO.2008.19.6618](https://doi.org/10.1200/JCO.2008.19.6618). [PubMed: [19289619](https://pubmed.ncbi.nlm.nih.gov/19289619/)].
- Kaufman B, Mackey JR, Clemens MR, Bapsy PP, Vaid A, Wardley A, et al. Trastuzumab plus anastrozole versus anastrozole alone for the treatment of postmenopausal women with human epidermal growth factor receptor 2-positive, hormone receptor-positive metastatic breast cancer: Results from the randomized phase III TAnDEM study. *J Clin Oncol.* 2009;27(33):5529–37. doi: [10.1200/JCO.2008.20.6847](https://doi.org/10.1200/JCO.2008.20.6847). [PubMed: [19786670](https://pubmed.ncbi.nlm.nih.gov/19786670/)].
- Molina MA, Codony-Servat J, Albanell J, Rojo F, Arribas J, Baselga J. Trastuzumab (Herceptin), a humanized anti-Her2 receptor monoclonal antibody, inhibits basal and activated Her2 ectodomain cleavage in breast cancer cells. *Cancer Res.* 2001;61(12):4744–9. [PubMed: [11406546](https://pubmed.ncbi.nlm.nih.gov/11406546/)].
- Nahta R, Esteva FJ. HER2 therapy: Molecular mechanisms of trastuzumab resistance. *Breast Cancer Res.* 2006;8(6):215. doi: [10.1186/bcr1612](https://doi.org/10.1186/bcr1612). [PubMed: [17096862](https://pubmed.ncbi.nlm.nih.gov/17096862/)]. [PubMed Central: [PMC1797036](https://pubmed.ncbi.nlm.nih.gov/PMC1797036/)].
- Dosio F, Brusa P, Cattel L. Immunotoxins and anticancer drug conjugate assemblies: The role of the linkage between components. *Toxins (Basel).* 2011;3(7):848–83. doi: [10.3390/toxins3070848](https://doi.org/10.3390/toxins3070848). [PubMed: [22069744](https://pubmed.ncbi.nlm.nih.gov/22069744/)]. [PubMed Central: [PMC3202854](https://pubmed.ncbi.nlm.nih.gov/PMC3202854/)].
- Kreitman RJ, Hassan R, Fitzgerald DJ, Pastan I. Phase I trial of continuous infusion anti-mesothelin recombinant immunotoxin SSI-P. *Clin Cancer Res.* 2009;15(16):5274–9. doi: [10.1158/1078-0432.CCR-09-0062](https://doi.org/10.1158/1078-0432.CCR-09-0062). [PubMed: [19671873](https://pubmed.ncbi.nlm.nih.gov/19671873/)]. [PubMed Central: [PMC2754261](https://pubmed.ncbi.nlm.nih.gov/PMC2754261/)].
- Allured VS, Collier RJ, Carroll SF, McKay DB. Structure of exotoxin A of *Pseudomonas aeruginosa* at 3.0-Ångstrom resolution. *Proc Natl Acad Sci U S A.* 1986;83(5):1320–4. doi: [10.1073/pnas.83.5.1320](https://doi.org/10.1073/pnas.83.5.1320). [PubMed: [3006045](https://pubmed.ncbi.nlm.nih.gov/3006045/)]. [PubMed Central: [PMC323067](https://pubmed.ncbi.nlm.nih.gov/PMC323067/)].
- Hwang J, Fitzgerald DJ, Adhya S, Pastan I. Functional domains of *Pseudomonas* exotoxin identified by deletion analysis of the gene expressed in *E. coli*. *Cell.* 1987;48(1):129–36. doi: [10.1016/0092-8674\(87\)90363-1](https://doi.org/10.1016/0092-8674(87)90363-1). [PubMed: [3098436](https://pubmed.ncbi.nlm.nih.gov/3098436/)].
- Siegal CB, Chaudhary VK, Fitzgerald DJ, Pastan I. Functional analysis of domains II, Ib, and III of *Pseudomonas* exotoxin. *J Biol Chem.* 1989;264(24):14256–61. [PubMed: [2503515](https://pubmed.ncbi.nlm.nih.gov/2503515/)].
- Kihara A, Pastan I. Analysis of sequences required for the cytotoxic action of a chimeric toxin composed of *Pseudomonas* exotoxin and transforming growth factor alpha. *Bioconjug Chem.* 1994;5(6):532–8. doi: [10.1021/bc00030a008](https://doi.org/10.1021/bc00030a008). [PubMed: [7873657](https://pubmed.ncbi.nlm.nih.gov/7873657/)].
- Fraser ME, Chernai MM, Kozlov YV, James MN. Crystal structure of the holotoxin from *Shigella dysenteriae* at 2.5 Å resolution. *Nat Struct Biol.* 1994;1(1):59–64. doi: [10.1038/nsb0194-59](https://doi.org/10.1038/nsb0194-59). [PubMed: [7656009](https://pubmed.ncbi.nlm.nih.gov/7656009/)].
- Jacewicz M, Clausen H, Nudelman E, Donohue-Rolfe A, Keusch GT. Pathogenesis of shigella diarrhea. XI. Isolation of a shigella toxin-binding glycolipid from rabbit jejunum and HeLa cells and its identification as globotriaosylceramide. *J Exp Med.* 1986;163(6):1391–404. doi: [10.1084/jem.163.6.1391](https://doi.org/10.1084/jem.163.6.1391). [PubMed: [3519828](https://pubmed.ncbi.nlm.nih.gov/3519828/)]. [PubMed Central: [PMC2188132](https://pubmed.ncbi.nlm.nih.gov/PMC2188132/)].
- Garred O, Dubinina E, Poleskaya A, Olsnes S, Kozlov J, Sandvig K. Role of the disulfide bond in Shiga toxin A-chain for toxin entry into cells. *J Biol Chem.* 1997;272(17):11414–9. doi: [10.1074/jbc.272.17.11414](https://doi.org/10.1074/jbc.272.17.11414). [PubMed: [9111051](https://pubmed.ncbi.nlm.nih.gov/9111051/)].
- O'Brien AD, Tesh VL, Donohue-Rolfe A, Jackson MP, Olsnes S, Sandvig K, et al. Shiga toxin: Biochemistry, genetics, mode of action, and role in pathogenesis. *Curr Top Microbiol Immunol.* 1992;180:65–94. [PubMed: [1324134](https://pubmed.ncbi.nlm.nih.gov/1324134/)].
- Fuller CA, Pellino CA, Flagler MJ, Strasser JE, Weiss AA. Shiga toxin subtypes display dramatic differences in potency. *Infect Immun.* 2011;79(3):1329–37. doi: [10.1128/IAI.01182-10](https://doi.org/10.1128/IAI.01182-10). [PubMed: [21199911](https://pubmed.ncbi.nlm.nih.gov/21199911/)]. [PubMed Central: [PMC3067513](https://pubmed.ncbi.nlm.nih.gov/PMC3067513/)].
- Grupka NL, Lear-Kaul KC, Kleinschmidt-DeMasters BK, Singh M. Epidermal growth factor receptor status in breast cancer metastases to the central nervous system. Comparison with HER-2/neu status. *Arch Pathol Lab Med.* 2004;128(9):974–9. doi: [10.1043/1543-2165\(2004\)128<974:EGFRS1>2.0.CO;2](https://doi.org/10.1043/1543-2165(2004)128<974:EGFRS1>2.0.CO;2). [PubMed: [15335267](https://pubmed.ncbi.nlm.nih.gov/15335267/)].
- Aziz SA, Pervez S, Khan S, Kayani N, Rahbar MH. Epidermal growth factor receptor (EGFR) as a prognostic marker: An immunohistochemical study on 315 consecutive breast carcinoma patients. *J Pak Med Assoc.* 2002;52(3):104–10. [PubMed: [12071064](https://pubmed.ncbi.nlm.nih.gov/12071064/)].
- Baloria U, Akhoun BA, Gupta SK, Sharma S, Verma V. In silico proteomic characterization of human epidermal growth factor receptor 2 (HER-2) for the mapping of high affinity antigenic determinants against breast cancer. *Amino Acids.* 2012;42(4):1349–60. doi: [10.1007/s00726-010-0830-x](https://doi.org/10.1007/s00726-010-0830-x). [PubMed: [21229277](https://pubmed.ncbi.nlm.nih.gov/21229277/)].
- Ghasemi A, Ranjbar R, Amani J. In silico analysis of chimeric TF, Omp31 and BP26 fragments of *Brucella melitensis* for development of a multi subunit vaccine candidate. *Iran J Basic Med Sci.* 2014;17(3):172–80. [PubMed: [24847419](https://pubmed.ncbi.nlm.nih.gov/24847419/)]. [PubMed Central: [PMC4016687](https://pubmed.ncbi.nlm.nih.gov/PMC4016687/)].
- Amala S. In silico analysis and 3D modeling of ASAH1 protein in farber lipogranulomatosis. *Adv Biotech.* 2010;10(6):6–8.
- Garnier J, Gibrat JF, Robson B. GOR method for predicting protein secondary structure from amino acid sequence. *Methods Enzymol.* 1996;266:540–53. doi: [10.1016/S0076-6879\(96\)66034-0](https://doi.org/10.1016/S0076-6879(96)66034-0). [PubMed: [8743705](https://pubmed.ncbi.nlm.nih.gov/8743705/)].

28. Zhang Y. I-TASSER server for protein 3D structure prediction. *BMC Bioinformatics*. 2008;**9**:40. doi: [10.1186/1471-2105-9-40](https://doi.org/10.1186/1471-2105-9-40). [PubMed: [18215316](https://pubmed.ncbi.nlm.nih.gov/18215316/)]. [PubMed Central: [PMC2245901](https://pubmed.ncbi.nlm.nih.gov/PMC2245901/)].
29. Guex N, Peitsch MC. SWISS-MODEL and the Swiss-PdbViewer: An environment for comparative protein modeling. *Electrophoresis*. 1997;**18**(15):2714–23. doi: [10.1002/elps.1150181505](https://doi.org/10.1002/elps.1150181505). [PubMed: [9504803](https://pubmed.ncbi.nlm.nih.gov/9504803/)].
30. Ahmad S, Gromiha M, Fawareh H, Sarai A. ASAView: Database and tool for solvent accessibility representation in proteins. *BMC Bioinformatics*. 2004;**5**:51. doi: [10.1186/1471-2105-5-51](https://doi.org/10.1186/1471-2105-5-51). [PubMed: [15119964](https://pubmed.ncbi.nlm.nih.gov/15119964/)]. [PubMed Central: [PMC420234](https://pubmed.ncbi.nlm.nih.gov/PMC420234/)].
31. Laskowski RA, MacArthur MW, Moss DS, Thornton JM. PROCHECK: A program to check the stereochemical quality of protein structures. *J Appl Crystallogr*. 1993;**26**(2):283–91. doi: [10.1107/s0021889892009944](https://doi.org/10.1107/s0021889892009944).
32. Mahboobi M, Sedighian H, Hedayati Ch M, Bambai B, Esmail Soofian S, Amani J. Applying bioinformatic tools for modeling and modifying type ii e. Coli l-asparaginase to present a better therapeutic agent/drug for acute lymphoblastic leukemia. *Int J Cancer Manag*. 2017;**10**(3). doi: [10.5812/ijcm.5785](https://doi.org/10.5812/ijcm.5785).
33. Kovtun YV, Goldmacher VS. Cell killing by antibody-drug conjugates. *Cancer Lett*. 2007;**255**(2):232–40. doi: [10.1016/j.canlet.2007.04.010](https://doi.org/10.1016/j.canlet.2007.04.010). [PubMed: [17553616](https://pubmed.ncbi.nlm.nih.gov/17553616/)].
34. Junutula JR, Raab H, Clark S, Bhakta S, Leipold DD, Weir S, et al. Site-specific conjugation of a cytotoxic drug to an antibody improves the therapeutic index. *Nat Biotechnol*. 2008;**26**(8):925–32. doi: [10.1038/nbt.1480](https://doi.org/10.1038/nbt.1480). [PubMed: [18641636](https://pubmed.ncbi.nlm.nih.gov/18641636/)].
35. Jiang H, Rugo HS. Human epidermal growth factor receptor 2 positive (HER2+) metastatic breast cancer: How the latest results are improving therapeutic options. *Ther Adv Med Oncol*. 2015;**7**(6):321–39. doi: [10.1177/1758834015599389](https://doi.org/10.1177/1758834015599389). [PubMed: [26557900](https://pubmed.ncbi.nlm.nih.gov/26557900/)]. [PubMed Central: [PMC4622301](https://pubmed.ncbi.nlm.nih.gov/PMC4622301/)].
36. Ahmad ZA, Yeap SK, Ali AM, Ho WY, Alitheen NB, Hamid M. scFv antibody: Principles and clinical application. *Clin Dev Immunol*. 2012;**2012**:980250. doi: [10.1155/2012/980250](https://doi.org/10.1155/2012/980250). [PubMed: [22474489](https://pubmed.ncbi.nlm.nih.gov/22474489/)]. [PubMed Central: [PMC3312285](https://pubmed.ncbi.nlm.nih.gov/PMC3312285/)].
37. Keshavarz M, Salimian J, Yaseri M, Bathaie SZ, Rezaie E, Aliramezani A, et al. Bioinformatic prediction and experimental validation of a PE38-based recombinant immunotoxin targeting the Fn14 receptor in cancer cells. *Immunotherapy*. 2017;**9**(5):387–400. doi: [10.2217/imt-2017-0008](https://doi.org/10.2217/imt-2017-0008). [PubMed: [28357912](https://pubmed.ncbi.nlm.nih.gov/28357912/)].
38. Imani-Fooladi AA, Yousefi F, Mousavi SF, Amani J. In silico design and analysis of TGFalphaL3-SEB fusion protein as "a new antitumor agent" candidate by ligand-targeted superantigens technique. *Iran J Cancer Prev*. 2014;**7**(3):152–64. [PubMed: [25250167](https://pubmed.ncbi.nlm.nih.gov/25250167/)]. [PubMed Central: [PMC4171824](https://pubmed.ncbi.nlm.nih.gov/PMC4171824/)].
39. Chen X, Zaro JL, Shen WC. Fusion protein linkers: Property, design and functionality. *Adv Drug Deliv Rev*. 2013;**65**(10):1357–69. doi: [10.1016/j.addr.2012.09.039](https://doi.org/10.1016/j.addr.2012.09.039). [PubMed: [23026637](https://pubmed.ncbi.nlm.nih.gov/23026637/)]. [PubMed Central: [PMC3726540](https://pubmed.ncbi.nlm.nih.gov/PMC3726540/)].